Structure
Article

# An Autoinhibited Noncanonical Mechanism of GTP Hydrolysis by Rheb Maintains mTORC1 Homeostasis

Mohammad T. Mazhab-Jafari,[1,2] Christopher B. Marshall,[1,2] Noboru Ishiyama,[1,2] Jason Ho,[1,2] Vanessa Di Palma,[1,2] Vuk Stambolic,[1,2,*] and Mitsuhiko Ikura[1,2,*]
[1]Department of Medical Biophysics, University of Toronto, Toronto, Ontario M5G 2M9, Canada
[2]Campbell Family Cancer Research Institute, Ontario Cancer Institute, Princess Margaret Cancer Center, University Health Network, Toronto, Ontario M5G 1L7, Canada
*Correspondence: vuks@uhnres.utoronto.ca (V.S.), mikura@uhnres.utoronto.ca (M.I.)
http://dx.doi.org/10.1016/j.str.2012.06.013

## SUMMARY

**Rheb, an activator of mammalian target of rapamycin (mTOR), displays low intrinsic GTPase activity favoring the biologically activated, GTP-bound state. We identified a Rheb mutation (Y35A) that increases its intrinsic nucleotide hydrolysis activity ~10-fold, and solved structures of both its active and inactive forms, revealing an unexpected mechanism of GTP hydrolysis involving Asp65 in switch II and Thr38 in switch I. In the wild-type protein this noncanonical mechanism is markedly inhibited by Tyr35, which constrains the active site conformation, restricting the access of the catalytic Asp65 to the nucleotide-binding pocket. Rheb Y35A mimics the enthalpic and entropic changes associated with GTP hydrolysis elicited by the GTPase-activating protein (GAP) TSC2, and is insensitive to further TSC2 stimulation. Overexpression of Rheb Y35A impaired the regulation of mTORC1 signaling by growth factor availability. We demonstrate that the opposing functions of Tyr35 in the intrinsic and GAP-stimulated GTP catalysis are critical for optimal mTORC1 regulation.**

## INTRODUCTION

Small GTPases act as molecular switches to regulate diverse cellular functions. When bound to guanosine triphosphate (GTP), they adopt an "on" conformation that elicits a biological response. GTP hydrolysis is accompanied by a conformational change into a GDP-bound "off" conformation. Cycling between the active and inactive states of each GTPase is a result of the intrinsic nucleotide hydrolysis and exchange rates, and regulatory proteins that catalyze these processes. GTPase-activating proteins (GAPs) stimulate GTP hydrolysis, whereas guanine nucleotide exchange factors (GEFs) mediate the displacement of GDP, allowing a new GTP molecule to bind (Bos et al., 2007). GTPase proteins possess either complete or partial catalytic machinery for hydrolysis of GTP. In most cases an electronegative group is used for stabilization/polarization of the hydrolytic water for in-line nucleophilic attack of the γ-phosphate (Li and Zhang, 2004; Maegley et al., 1996). In most Ras and Rho subfamily GTPases, this is achieved by the carboxamide oxygen of a conserved Gln in a dynamic loop called switch II. Ras and Rho GAPs work by stabilizing this Gln in a catalytic conformation, whereas an Arg residue referred to as an "Arginine finger" neutralizes the developing negative charge on the α- and β-phosphates of GTP (Scheffzek et al., 1997). In other systems, such as Rap-RapGAP, a catalytic asparagine is provided in *trans* by the GAP (Scrima et al., 2008).

Ras homolog enriched in brain (Rheb) is a key regulator of the mammalian target of rapamycin (mTOR) complex 1 (mTORC1) signaling pathway (Dunlop et al., 2009; Inoki et al., 2003). Rheb-GTP promotes phosphorylation of mTORC1 targets, resulting in enhanced protein translation and cellular growth (Garami et al., 2003). Rheb has an unusually slow intrinsic GTPase activity, which is regulated by the GAP activity of tuberous sclerosis complex 2 (TSC2), a tumor suppressor frequently inactivated in human patients with the tumor predisposition syndrome tuberous sclerosis (Garami et al., 2003; Tee et al., 2003). Rheb overexpression has been observed in certain cancer cell lines (Eom et al., 2008; Im et al., 2002; Nardella et al., 2008), and constitutively activated Rheb mutants can induce oncogenic transformation in cell culture (Jiang and Vogt, 2008). The low intrinsic GTPase activity of Rheb has been attributed to the catalytically incompetent conformation of Gln64 (Yu et al., 2005), which is homologous to Ras Gln61, but does not participate in GTP hydrolysis (Li et al., 2004; Marshall et al., 2009). TSC2GAP is thought to utilize Asn1643 to promote GTP hydrolysis by substituting for Gln64 in an "Asn thumb"-type mechanism (Inoki et al., 2003; Marshall et al., 2009) similar to that of RapGAP (Scrima et al., 2008).

Here, utilizing site-directed mutagenesis, crystallography, and real-time NMR-based GTPase assays, we discovered that Rheb Tyr35, a residue that is highly conserved across the small GTPase superfamily (Wennerberg et al., 2005), maintains the high activation state of Rheb by inhibiting intrinsic GTP hydrolysis. Mutation of this residue substantially accelerated intrinsic nucleotide hydrolysis through a catalytic mechanism that did not require Gln64 but also conferred resistance to the activity of TSC2. Crystal structures of Rheb Y35A led us to identify the backbone carbonyl of Thr38 and side chain of Asp65 as

 

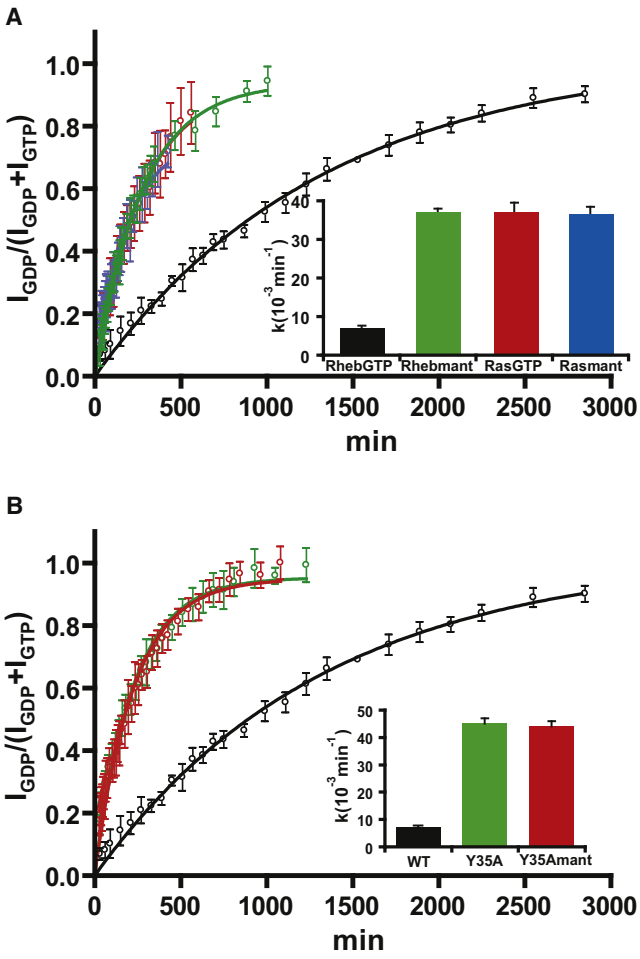


**Figure 1. Rapid Hydrolysis of mantGTP by Rheb Is Related to Autoinhibitory Role of Tyr35**

(A) Hydrolysis of GTP or mantGTP by Rheb (black and green, respectively) and Ras (red and blue, respectively) is shown. Reaction rates derived by curve fitting are presented in the insets.

(B) Hydrolysis of GTP by WT Rheb (black), and GTP and mantGTP by Rheb Y35A (green and red, respectively) is presented.

Error bars associated with data points in the curves represent SD of the fraction GDP reported by several residues. Error bars in the histograms represent the uncertainty associated with rates derived from curve fitting.

See also Figures S1 and S3.

candidate residues that contribute to the intrinsic GTPase activity. Mutagenesis studies confirm that Asp65 contributes significantly to the intrinsic GTPase activity of both wild-type (WT) Rheb and the Y35A mutant. Furthermore, Asp65 was absolutely essential for the sensitivity of Rheb to the GAP activity of TSC2, whereas Gln64 was dispensable. Consistent with the in vitro data, expression of Rheb Y35A and D65A mutants in mammalian cells affected transduction of growth factor signals to mTORC1. Taken together, our observations reveal an efficient noncanonical mechanism of GTP hydrolysis by Rheb and suggest that autoinhibition of catalysis maintains Rheb in its highly activated state upon growth factor stimulation, which is necessary for the proper signal transduction to mTORC1.

## RESULTS

### Rheb Y35 Inhibits Intrinsic GTPase Activity

We previously showed that fluorescent-tagged nucleotides can alter the hydrolysis and exchange rates governing the GTPase cycle (Mazhab-Jafari et al., 2010). The most striking example we observed was that 2′-/3′-O-(N′-Methylanthraniloyl) (mant) GTP was hydrolyzed by Rheb ~10-fold faster than GTP. This is not an intrinsic property of the modified nucleotide because the mant moiety inhibited GTP hydrolysis by RhoA and did not affect hydrolysis by Ras. The rate of mantGTP hydrolysis by Rheb is similar to that of Ras (Figure 1A), indicating that Rheb has a latent capacity for efficient catalysis. Interestingly, however, the rapid hydrolysis of mantGTP was independent of Rheb Gln64 (Mazhab-Jafari et al., 2010). The position of the fluorophore in a structure of Ras bound to a nonhydrolyzable analog of mantGTP (Scheidig et al., 1995) suggested that it may interact with the phenol ring of Tyr35 in switch I of Rheb. Remarkably, mutation of Tyr35 to Ala recapitulated the mant effect, increasing the rate of GTP hydrolysis by an order of magnitude (Figure 1B). Furthermore, the mant tag had no further effect on the catalytic activity of Rheb Y35A, suggesting that the mutation and the fluorophore stimulate hydrolysis through the same mechanism (Figure 1B). These observations indicate that Tyr35 autoinhibits the intrinsic GTPase activity of Rheb.

### Structural Basis for the Tyr35 Autoinhibitory Function

We crystallized GDP-bound Rheb Y35A in the presence of excess GMPPNP (a nonhydrolyzable analog of GTP), and to our surprise, the asymmetric unit contained two molecules of Rheb: one bound to GDP and one to GMPPNP (Figures 2A–2C; Table 1). The overall protein fold is very similar to WT Rheb (Yu et al., 2005) (backbone rmsd of 0.44 Å) with a few key differences. The nucleotide-binding pocket is completely solvent exposed in the GMPPNP-bound structure of Rheb Y35A, whereas in the WT protein the triphosphate group of the nucleotide is shielded from the solvent by the phenol ring of Tyr35, which forms a hydrogen bond with the γ-phosphate. In addition the γ-phosphate is 0.5 Å closer to Thr38 in the absence of Tyr35 (Figure 2D), which in the WT structure "pulls" the γ-phosphate toward the middle of switch I. Interestingly, the hydrolytic water is closer to the backbone carbonyl of Thr38 in the mutant (2.7 versus 3.8 Å in the WT protein) (Figure 2D), placing it in a more electron-rich environment that may enhance its polarization for an in-line nucleophilic attack to the γ-phosphate. It has been proposed that the corresponding backbone carbonyl of Ras (Thr35) contributes to the stabilization/activation of the catalytic water during intrinsic GTP hydrolysis (Buhrman et al., 2010; Frech et al., 1994). Comparison of our structure with that of WT Rheb indicates that Tyr35 pulls the γ-phosphate and catalytic water away from the Thr38 carbonyl, thus reducing its catalytic contribution.

Switch I of Rheb Y35A does not undergo any substantial conformational change upon nucleotide hydrolysis, whereas this region of the WT protein exhibits a large structural change mediated by an interaction between Tyr35 and the γ-phosphate (Yu et al., 2005) (Figures 2E and 2F). It was hypothesized that a similar nucleotide-dependent rearrangement of Rap Tyr32 would be energetically unfavorable to the GTPase reaction (Cherfils et al., 1997), consistent with our observation that

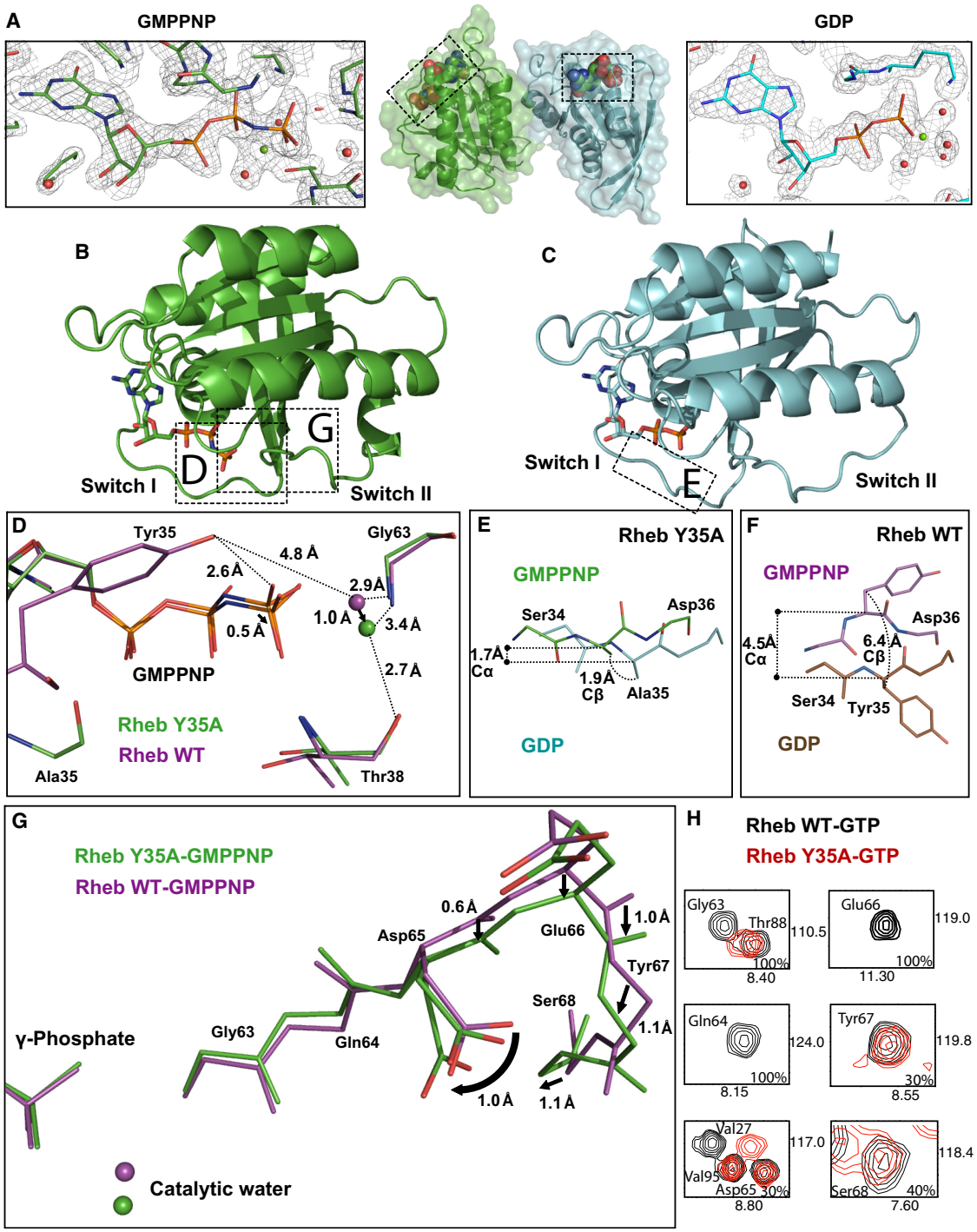


**Figure 2. Structure and Dynamics of Rheb Y35A**

(A) Asymmetric unit and electron density of nucleotide substrates are demonstrated. The asymmetric unit of the Rheb Y35A crystal containing one GDP-bound (cyan) and one GMPPNP-bound (green) Rheb molecule is shown in the center. $2F_o$-$F_c$ electron density maps at 1.5σ of the nucleotide-binding site with GMPPNP (left) fitted into one Rheb Y35A molecule and GDP (right) in the second molecule of the crystal asymmetric unit is illustrated. Areas bounded by dashed-line rectangles are expanded on the left and right.

(B) Ribbon model of GMPPNP-bound Rheb Y35A is shown. Areas bounded by dashed-line rectangles are expanded in (D) and (G), as indicated.

(C) Ribbon model of GDP-bound Rheb Y35A in the same orientation as (B) is presented. Area bounded by dashed-line rectangle is expanded in (E).

(D)–(G) show overlays of GMPPNP- or GDP-bound Rheb Y35A (colored as above) and WT Rheb in complex with GMPPNP$^{(1XTR)}$ (magenta) or GDP$^{(1XTQ)}$ (gray), as indicated. (D) Mutation of Tyr35 affects the position of the catalytic water (spheres) and γ-phosphate with respect to the carbonyl of Thr38. (E) Minor conformational change of Ala35 in the Rheb mutant upon GTP hydrolysis. The Ala35 Cα and Cβ translocation distances from the GMPPNP-bound form to the GDP-bound form are shown with dotted lines. (F) Major conformational rearrangement of WT Rheb Tyr35 upon GTP hydrolysis, with translocations indicated as

**Table 1. Data Collection and Refinement Statistics**

| | Rheb Y35A |
|---|---|
| Data Collection | |
| Space group | $P\,2\,2_1\,2_1$ |
| Cell dimensions | |
| *a*, *b*, *c* (Å) | 57.2, 69.9, 79.2 |
| α, β, γ (°) | 90, 90, 90 |
| Resolution (Å) | 46.4–2.0 (2.07–2.0)[a] |
| $R_{sym}$ | 9.3 (41.2) |
| $I/\sigma I$ | 20.7 (4.6) |
| Completeness (%) | 99.7 (100) |
| Redundancy | 7.0 (6.6) |
| Refinement | |
| Resolution (Å) | 26.9–2.0 |
| No. of reflections | 21,742 |
| $R_{work}/R_{free}$ | 16.2/21.4 |
| No. of atoms | |
| Protein | 2,766 |
| Ligand/$Mg^{2+}$ ion | 62/2 |
| Water | 252 |
| B factors | |
| Protein | 26.3 |
| Ligand/$Mg^{2+}$ ion | 21.6/24.2 |
| Water | 30.3 |
| Rmsds | |
| Bond lengths (Å) | 0.007 |
| Bond angles (°) | 1.14 |
| Ramachandran statistics | |
| Most favorable regions (%) | 96.7 |
| Allowed regions (%) | 3.3 |
| Disallowed regions (%) | 0 |

Values in parentheses are for highest-resolution shell.
[a]Data set was collected from one crystal.

nucleotide hydrolysis is accelerated by a mutation that disrupts this conformational change.

## Identification of a Catalytic Residue for GTP Hydrolysis

Previous work has shown that Gln64, corresponding to the catalytic Gln61 of Ras, is not involved in GTP hydrolysis by WT Rheb (Inoki et al., 2003; Li et al., 2004; Marshall et al., 2009). Likewise, Gln64 remains in a noncatalytic conformation in the structure of Rheb Y35A (see Figure S1A available online) and is not required for the accelerated hydrolysis of GTP by Rheb Y35A (Figures S1D and S2A). Because the catalytic residues of other small GTPase superfamily members are found in the N terminus of switch II, we examined this region for residues with electronegative side chains that may contribute to the hydrolytic reaction. Immediately downstream of Gln64 are two residues with acidic side chains: Asp65 and Glu66 (Figure 2G). The crystal structure of Rheb Y35A shows that the backbone of the N-terminal loop of switch II of this mutant is displaced by an average of 1 Å toward the nucleotide-binding pocket relative to the WT, which brings the side-chain carboxylate of Asp65 closer to the nucleotide by 1 Å: average $Asp65O_{\delta1,2}{}^{WT}$ − average $Asp65O_{\delta1,2}{}^{Y35A}$ (Figure 2G). Mutation of Asp65 to Ala reduced the intrinsic hydrolysis of Rheb Y35A by more than 60% and that of WT by 30% (Figure 3A), as did the conservative substitution of Asp65 by Asn (Figure S2B). On the other hand, mutations of Glu66 had no effect on intrinsic GTPase activity (Figure S2C), consistent with its perpendicular orientation away from the nucleotide (Figure 2G). We also tested all other residues found within 10 Å of the hydrolytic water in the Rheb Y35A structure that could potentially provide (1) a negative charge to activate this water molecule, or (2) a positive charge to stabilize the β- and γ-phosphates in the transition state for hydrolysis (Figure S1). There was no change in the rate of intrinsic nucleotide hydrolysis associated with R15G, S16A, or D36A mutations (Figures S1B, S1C, and S1E). The only other charged residues within 10 Å of the hydrolytic water are Lys19 and Asp60 of the highly conserved G1 and G3 box motifs, respectively. The Rheb K19A mutant failed to express, presumably due to impaired nucleotide binding, and D60A was highly unstable and could not be loaded with GTP, consistent with the role of this residue in $Mg^{2+}$ coordination (Yu et al., 2005). These data strongly suggest that Asp65 is the sole candidate for a catalytic residue in Rheb. Notably, carboxylates are more potent nucleophiles than carboxamides, and consistently, the Q61E substitution increased the GTPase activity of Ras (Frech et al., 1994).

In the structure of WT Rheb, the carboxylate of Asp65 is 12 Å (average $Asp65O_{\delta1,2}$) from the γ-phosphate in a single conformation, whereas the electron density of Rheb Y35A indicates that Asp65 exists in two conformations, 11.0 and 12.0 Å from the γ-phosphate, respectively (Figure S1F). By comparison the catalytic carboxamide of Ras ($Gln61O_{\varepsilon}$) has been found at distances varying from 4.7 to 12.2 Å from the γ-phosphate (median distance of 8.1Å) (Figure S3A) in available crystallographic snapshots, consistent with the dynamic nature of switch II determined by NMR studies (Ito et al., 1997). Thus, despite its established role as a catalytic residue (Frech et al., 1994), Gln61 is rarely found in a catalytically competent conformation in Ras crystal structures, presumably because this state is transient and energetically unfavorable (Fraser et al., 2011; Grant et al., 2009). Similarly, our Y35A structure and the previous WT Rheb structure (Yu et al., 2005) both appear to be energetically stable states, with the conformations of Asp65 stabilized primarily by ionic and polar interactions with the Arg15 and Ser68 side chains, which are also found in two alternate conformations in our structure (Figure S1F). Interestingly, comparison of WT and

in (E). (G) Position of switch II residues relative to the nucleotide-binding site in the activated form of WT Rheb versus that of the Y35A mutant. The backbone of N-terminal switch II residues Gly63-Ser68 and side chains of Asp65 and Glu66 are shown. Two conformations were observed for the Asp65 side chain.
(H) $^{1}H$-$^{15}N$ HSQC spectra illustrating cross-peaks from switch II residues in WT Rheb (black) and Rheb Y35A (red) in complex with GTP. The panel showing Ser68 is illustrated at a higher contour level for clarity. The reduction in height of the peak from the mutant relative to the WT peak is indicated as a percentage at the bottom of each panel in which it is measurable. The full spectra are shown in Figure S4A.
See also Figures S3 and S4.

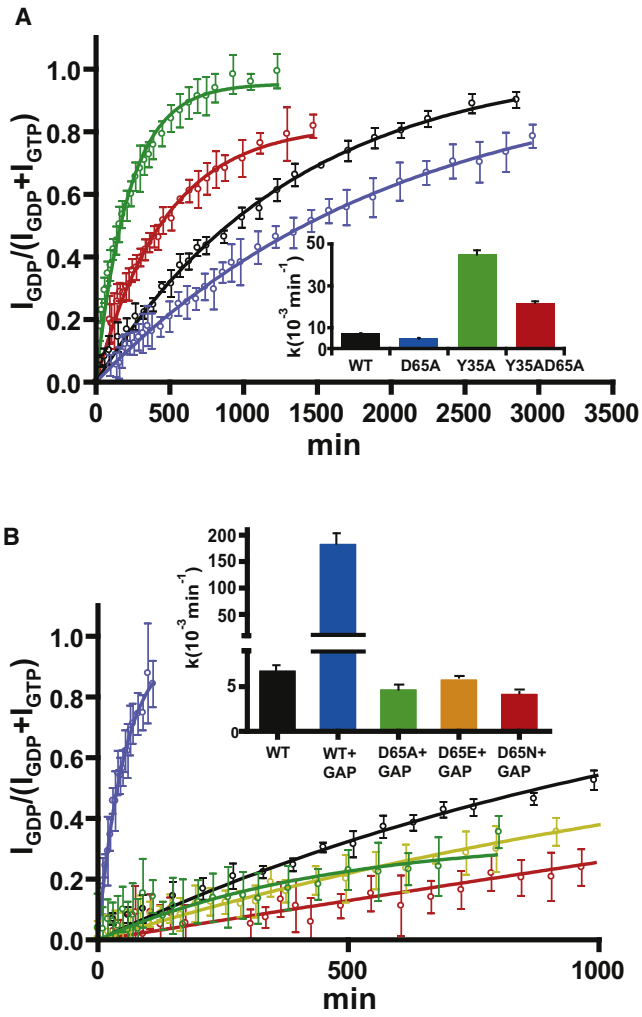


**Figure 3. Role of Asp65 in Intrinsic and GAP-Mediated GTP Hydrolysis by Rheb**

(A) Hydrolysis of GTP by WT Rheb (black), the mutants D65A and Y35A (blue and green, respectively), as well as the double-mutant Y35A-D65A (red) is illustrated. Reaction rates derived by curve fitting are presented in the insets.
(B) Sensitivity of WT Rheb and Asp65 mutants to TSC2GAP-stimulated GTP hydrolysis is shown. WT, WT+GAP, D65A+GAP, D65E+GAP, and D65N+GAP are shown with black, blue, green, yellow, and red, respectively.
Error bars associated with data points in the curves represent SD of the fraction GDP reported by several residues. Error bars in the histograms represent the uncertainty associated with rates derived from curve fitting.
See also Figures S1, S2, and S5.

Y35A $^{1}H$-$^{15}N$ heteronuclear single-quantum coherence (HSQC) spectra revealed increased line broadening for residues in the P loop and the N terminus of switch II of GTP-bound Rheb Y35A (Figures 2H and S4A), suggesting elevated dynamics in μs-ms timescale. This could allow the N terminus of switch II to sample alternate conformations closer to the nucleotide and the catalytic water. The elevated dynamics of the N-terminal region of switch II and its proximity to the nucleotide-binding site in Rheb Y35A is consistent with the greater impact on catalysis of Asp65 mutations in the Y35A mutant than in WT Rheb (Figure 3A). Hence, in addition to affecting the orientation of the nucleotide and hydrolytic water, Tyr35 may reduce the intrinsic GTPase activity of Rheb by restricting the dynamics of switch II and displacing it from the nucleotide-binding site. Relative to Ras, the catalytic Gln residues of Rho subfamily GTPases were found closer to the γ-phosphate (median distance of 5.5Å) (Figures S3A and S3C), which may contribute to their faster intrinsic nucleotide hydrolysis rate (Mazhab-Jafari et al., 2010). On the other hand, Gln63, which was recently proposed to be a noncanonical catalytic residue of Rap in GAP1$^{IP4BP}$-mediated GTP hydrolysis (Sot et al., 2010), is found with a median distance of 11.8 Å from the γ-phosphate in structures of free Rap (Figure S3A), consistent with the slow nucleotide hydrolysis of this GTPase.

In Ras, Gly12, Gly13, and Gln61 are the major sites of oncogenic mutations. Mutation of Ras Gly12 to any other residue hinders GTP hydrolysis by sterically occluding access of the catalytic residue Gln61 to the hydrolytic water and nucleotide (Krengel et al., 1990). However, Rheb has an Arg in this position, and its mutation to Gly (R15G) does not increase the catalytic activity of Rheb Y35A (Figure S1E) or WT (Im et al., 2002; Li et al., 2004; Marshall et al., 2009; Yamagata et al., 1994). The distinctive impact of P loop residues on the activities of Ras and Rheb lends further support to the different molecular mechanisms of action of these two closely related GTPase homologs.

## Involvement of Rheb's Asp65 and Tyr35 in TSC2GAP-Mediated GTP Hydrolysis

Mutation of the solvent-exposed residue Asp65 to Ala (D65A) did not perturb the structure of Rheb, on the basis of minimal and localized chemical shift perturbations in the $^{1}H$-$^{15}N$ HSQC spectra that were mainly confined to switch II (Figure S5), but totally abolished the susceptibility of Rheb to the GAP activity of TSC2 (Figure 3B). Furthermore, even conservative mutations of Asp65 (D65E/N) rendered Rheb totally insensitive to the activity of TSC2GAP. The strict requirement for the geometry and charge of this side chain suggest that it might be a critical catalytic residue for the GAP-mediated hydrolysis reaction. We also tested the sensitivity of the GTPase activity of Rheb Y35A to the action of TSC2GAP and found that the GTPase activity of this mutant was not further stimulated by the addition of the GAP domain of TSC2 (Figure 4A). An analogous mutation (Y32A) impaired the sensitivity of Rap GTPase to the function of RapGAP (Brinkmann et al., 2002; Scrima et al., 2008); however, a conservative mutation (Y32F) was tolerated. Interestingly, the Y35F mutation was sufficient to render Rheb insensitive to the function of the TSC2GAP (Figure 4B), highlighting differences in the details of molecular recognition in these two homologous systems.

## Thermodynamic Basis for the Tyr35 Autoinhibitory Function

To better understand the energetic basis of Tyr35 autoinhibition, we analyzed the thermodynamics of the GTP hydrolysis reaction using an Arrhenius plot (Figure S6). This powerful technique allows one to extract energetic parameters, such as enthalpy, entropy, and free energy, from the highly unstable and low-populated transition state of an enzymatic reaction. The increased catalytic activity of Rheb Y35A was associated with a large

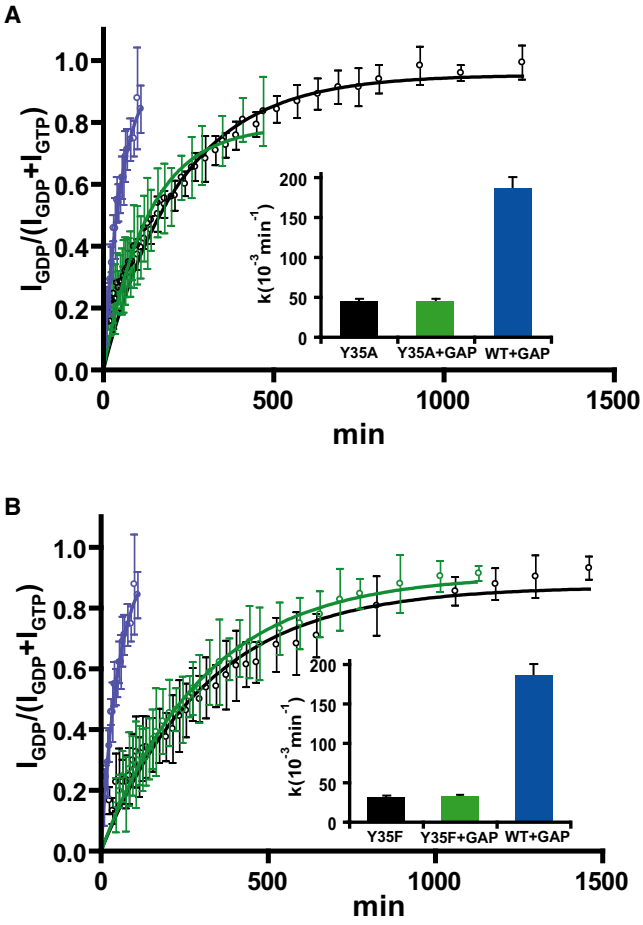


**Figure 4. Tyr35 Hydroxyl Is Required for TSC2GAP-Assisted GTP Hydrolysis**

(A) Intrinsic and GAP-catalyzed GTP hydrolysis by Rheb Y35A is presented.

(B) Intrinsic and GAP-catalyzed GTP hydrolysis by Rheb Y35F is demonstrated. In both graphs the GTPase activities of mutant Rheb with and without TSC2GAP are shown in black and green, respectively, and the TSC2GAP-catalyzed GTP hydrolysis by WT Rheb is shown in blue.

Error bars associated with data points in the curves represent SD of the fraction GDP reported by several residues. Error bars in the histograms represent the uncertainty associated with rates derived from curve fitting. See also Figure S4.

reduction in the activation enthalpy for GTP hydrolysis (Figure S6; Table 2). However, the activation entropy was also reduced (unfavorable contribution), resulting in a modest decrease in the overall activation free energy of the nucleotide hydrolysis reaction in the mutant. Because there is a buildup of negative charge on the β-γ-bridging oxygen during GTP hydrolysis (Allin et al., 2001; Cepus et al., 1998; Du et al., 2000), the proximity of the electron-rich phenol ring of Rheb Tyr35 could destabilize the transition state, which is consistent with the reduction in activation enthalpy associated with mutation of this residue. Interestingly, the Arg fingers of Ras- and Rho-GAPs accelerate nucleotide hydrolysis of their cognate GTPases by providing positive charge in a position equivalent to that of Rheb Tyr35. Another contribution to the enthalpic term may come from the strengthened hydrogen bond between the Thr38 carbonyl in the mutant and the repositioned catalytic water, which may be more reactive toward the γ-phosphate (Frech et al., 1994).

**Table 2. Summary of Thermodynamic Activation Parameters Calculated for GTP Hydrolysis by Rheb WT and Mutants**

| Protein | WT | Y35A | Y35F | Y35A-D65A | D65A | TSC2GAP[a] |
|---|---|---|---|---|---|---|
| $\Delta H^{\ddagger}$ | 86.0 | 52.3 | 52.7 | 55.6 | 87.0 | 41.3 |
| $T\Delta S^{\ddagger}$ | −13.5 | −43 | −43.3 | −41.6 | −13.3 | −51.8 |
| $\Delta G^{\ddagger}$ | 99.5 | 95.3 | 96.0 | 97.2 | 100.3 | 93.1 |

Free energy of activation ($\Delta G^{\ddagger}$), activation enthalpy ($\Delta H^{\ddagger}$), and activation entropy ($T\Delta S^{\ddagger}$) are in kJ/mol. T is set to 298 K in the equation $\Delta G^{\ddagger} = \Delta H^{\ddagger} - T\Delta S^{\ddagger}$. See also Figure S6.

[a]Values from Marshall et al. (2009).

The larger negative value of $\Delta S^{\ddagger}$ for Rheb Y35A indicates that formation of the transition state requires the mutant to undergo a larger increase in "order" than the WT protein. In the crystal structure of WT Rheb-GMPPNP, a hydrogen bond between the hydroxyl of Tyr35 and the γ-phosphate of GMPPNP stabilizes switch I, contributing to the order of the ground state. Disruption of this contact by mutation of Tyr35 increases the disorder in switch I, as illustrated by partial spectral broadening of peaks from residues 27–30 of GTP-bound Rheb Y35A (Figure S4). Thus, assembly of the ordered transition state from the more flexible Rheb Y35A ground state would be more entropically unfavorable. The conservative mutation Y35F increased intrinsic hydrolysis almost as much as Y35A with similar thermodynamic effects (Figure S6; Table 2), suggesting that the H bond between the hydroxyl of Tyr35 and the γ-phosphate is critical for the autoinhibition of Rheb's GTPase activity. It is very interesting to note that the thermodynamic landscape of intrinsic GTP hydrolysis in the Y35A mutant (reduced activation enthalpy with an entropic penalty) is similar to that reported for TSC2GAP-mediated GTP hydrolysis in WT Rheb (Marshall et al., 2009), suggesting that TSC2GAP may promote hydrolysis in part by disrupting the electrostatic contact between Tyr35 and the γ-phosphate. Consistent with this hypothesis, the increased rate of GTP hydrolysis by the Rheb Y35A/Y35F mutants is not further accelerated by the addition of the GAP (Figure 4). The larger reduction of the activation enthalpy by TSC2GAP-mediated catalysis compared to Y35A mutation suggests that the GAP provides additional stimulatory electrostatic contributions to GTP hydrolysis, perhaps via complementation of the intrinsic catalytic machinery by the Asn thumb. On the other hand the larger unfavorable reduction in entropy of the GAP-mediated reaction could be due to complex formation between Rheb and the GAP domain of TSC2.

Mutation of Asp65 substantially impairs the stimulatory effect of the Y35A mutation on intrinsic hydrolysis; hence, we measured the thermodynamic parameters of the transition state for the Rheb double-mutant Y35A-D65A (Table 2). Mutation of Asp65 increased the activation enthalpy ($\Delta H^{\ddagger}$) of Rheb Y35A, indicating that the negatively charged carboxylic acid side chain of Asp65 stabilizes the transition state because the enthalpic term originates primarily from electrostatic interactions (Kötting and Gerwert, 2004). In Ras the enthalpic contribution to hydrolysis was attributed to the charge shift from the γ- toward the β-phosphate (Kötting and Gerwert, 2004). We propose that

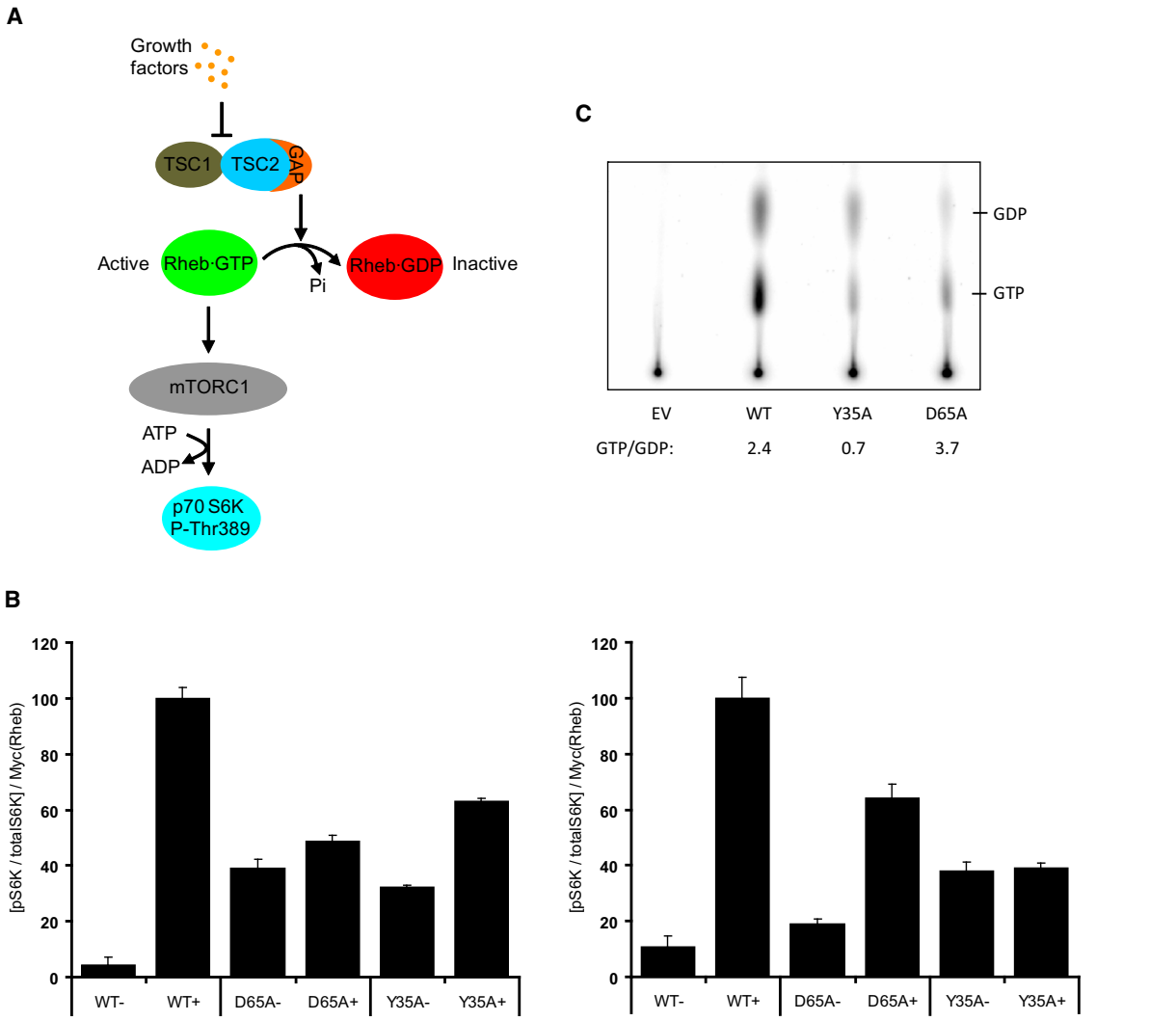


**Figure 5. Mutations of Rheb Catalytic and Autoinhibitory Residues Impact Rheb's Activation Level and mTORC1 Phosphorylation of p70 S6K**

(A) Signaling pathway by which growth factors stimulate mTORC1 phosphorylation of p70 S6K is illustrated.

(B) Normalized values of p70 S6K phosphorylation for cells starved (−) or stimulated (+) with serum and insulin for 15 min (left) or 6 hr (right) are shown as bar graphs. The background intensity was used as estimation for the error in the intensity measurements and propagated appropriately throughout division. More details are described in Experimental Procedures. Representative western blots are shown in Figure S7.

(C) Rheb nucleotide loading monitored in HEK293 cells with $^{32}$P-labeling experiment as described in Experimental Procedures is presented.

See also Figure S7.

electrostatic interactions between Rheb Asp65 and the nucleotide similarly shift charge in the transition state to promote hydrolysis. Interestingly, Tyr35 reduces the enthalpic contribution of Asp65 to GTP hydrolysis, $\Delta\Delta H^{\ddagger(Y35A\text{-}Y35A,D65A)} > \Delta\Delta H^{\ddagger(WT\text{-}D65A)}$ (Table 2), which is consistent with our kinetic data (Figure 3A).

## Regulation of mTORC1 by Growth Factors Involves the Noncanonical Catalytic and Autoinhibitory Mechanisms

To investigate the role of Rheb's catalytic machinery, and its autoinhibition, in the activation of mTORC1, HeLa cells were transfected with WT Rheb or the Y35A or D65A mutants. Phosphorylation of p70 S6K Thr389, a measure of mTORC1 signaling throughput (Figure 5A), was monitored by immunoblotting, upon growth factor starvation, as well as 15 min and 6 hr after growth factor stimulation (Figures 5B and S7). Following growth factor stimulation, when the TSC1/TSC2 complex is downregulated (Benvenuto et al., 2000; Chong-Kopera et al., 2006), mutation of Rheb Tyr35 to Ala reduced the activation of mTORC1, as evidenced by slightly lower p70 S6K phosphorylation despite higher Rheb Y35A expression compared to Rheb WT, an effect made more apparent with longer stimulation (Figures 5B and S7). Remarkably, in the absence of stimuli upon serum starvation, Rheb Y35A led to a significant increase in mTORC1 activity, as did the expression of the GAP-resistant mutant Rheb D65A (Figure 5B). Mutation of Asp65 (but not Tyr35) perturbed the chemical shift of the neighboring switch II residue Tyr67 (Figures S4A and S5), previously shown to be critical for activation of mTORC1 (Long et al., 2007), which may affect

the ability of Rheb D65A to fully activate mTORC1. This may explain the fact that under conditions of growth factor stimulation, Rheb D65A induced less S6K phosphorylation than the WT protein, despite its reduced intrinsic GTPase activity (Figure 5B).

Guanine nucleotide loading of WT Rheb and the mutants in vivo was determined by their immunoprecipitation from HEK293 cells metabolically labeled with $^{32}$P-orthophosphate and nucleotide resolution by thin-layer chromatography (Figure 5C). Consistent with its increased GTPase activity, Rheb Y35A displayed reduced loading of GTP, whereas Rheb D65A showed modestly increased GTP loading. Reflected in the elevated loading of WT Rheb with GTP (Figure 5C), the overabundance of transfected Rheb proteins likely negates the effects of endogenous TSC2 on the overexpressed Rheb mutants in this cell line. Although the lower GTP loading of Rheb Y35A indicates higher intrinsic hydrolysis rate than that of the WT protein, modestly increased GTP loading of D65A signifies the autoinhibitory effects of Tyr35 on Asp65's contribution to intrinsic catalysis, consistent with their in vitro behavior (Figure 3A).

## DISCUSSION

GTPases are versatile molecular switches that utilize surprisingly diverse mechanisms to mediate the interconversion between the active and inactive states. The study presented here illustrates how Rheb evolved a GTP hydrolysis mechanism drastically different from its close homolog H-Ras. Rheb employs an autoinhibitory mechanism to maintain a high activation state in cells essential for the proper maintenance of mTORC1 signaling and cellular growth.

The autoinhibitory mechanism functions via an interaction between Rheb Tyr35-OH and the γ-phosphate of GTP, which hinders GTP hydrolysis. Interestingly, our investigation of this inhibitory mechanism led to the elucidation of an unusual Rheb catalytic mechanism involving Asp65, which is one position downstream of the canonical catalytic Gln, equivalent to Ras Gln61 and Rho Gln63. In the canonical mechanism the catalytic water is activated/stabilized by interaction with an electronegative group, the carboxamide oxygen of a glutamine, provided either in *cis* or *trans* (Bos et al., 2007). Although an equivalent residue (Gln64) is present in the sequence of Rheb switch II, our work demonstrates that the catalytic function is carried out by the adjacent Asp65.

A Tyr residue in switch I is highly conserved among the GTPase superfamily; however, the functional role of this residue varies. For example in RhoA, Tyr34 stimulates intrinsic hydrolysis, presumably by stabilizing the catalytic conformation of Gln63 in switch II, whereas Ras Tyr32 is solvent exposed and does not impact the intrinsic hydrolysis (Figure S3). In Rheb, Tyr35 counters the contribution of Asp65 to catalysis by restricting the dynamics of switch II and reducing its access to the catalytic site (Figure 6). Severe peak broadening was observed for the amides of Gly63, Gln64, Asp65, and Glu66 in the $^{1}$H-$^{15}$N HSQC spectrum of the Y35A mutant (Figure 2H), presumably the result of disrupting the H bond network from Tyr35 to the amide of Gly63 through the catalytic water and the γ-phosphate (Figure 2D). Moreover, Tyr35 restricts the position of the hydrolytic water and reduces its polarization by the carbonyl of Thr38, which is thought to promote hydrolysis (Buhrman et al., 2010; Frech et al., 1994). The residual catalytic activity found in Rheb D65A may reflect the stimulatory effect of the Thr38 backbone carbonyl in polarization and/or stabilization of the hydrolytic water. Upon mutation of Tyr35, Asp65 adopts two conformations, one of which is more proximal (relative to the WT) to the nucleotide-binding site and appears better positioned for hydrolysis (Figure 2G), consistent with our finding that mutation of Asp65 has a greater impact on the catalytic activity of Rheb Y35A than that of WT (Figure 3A). On the basis of the multiple crystallographic conformations of Asp65, and the NMR peak broadening, we propose that in both WT and Y35A Rheb, switch II exists in an ensemble of conformations, some of which allow Asp65 to adopt a catalytic conformation closer to the nucleotide.

Structural evidence implicating Asp as a catalytic residue exists for at least one other member of the GTPase superfamily, the signal recognition particle (SRP) Ffh/FtsY (Focia et al., 2004), which is a large dimeric prokaryotic GTPase that is highly divergent from the Ras family. Nevertheless, to our knowledge, a catalytic Asp has not been previously reported within the Ras subfamily. On the other hand the inhibitory role for a switch I Tyr we discovered in Rheb may be relevant in inhibiting the intrinsic hydrolytic machinery in certain other GTPases, such as Ran (Brucker et al., 2010).

Our structural analysis of Rheb also shed further light on the mechanism of TSC2GAP-mediated hydrolysis of GTP. We propose that whereas providing an Asn thumb as a means of accelerating catalysis, TSC2GAP may also stimulate the GTPase activity of Rheb by relieving autoinhibition and aligning Rheb's catalytic machinery (Figure 6C). Interaction of TSC2 with Rheb switch I may disrupt the electrostatic contact between Tyr35 and the γ-phosphate, reducing the autoinhibitory effect of this residue on GTP hydrolysis, explaining the functional and thermodynamic similarities between WT Rheb in the presence of the TSC2GAP and the Rheb Y35A mutant alone. A common theme in GAP-stimulated GTP hydrolysis is repositioning of the N terminus of switch II relative to the nucleotide-binding site to allow for efficient catalysis. For example the RanGAP Asn thumb serves to properly orient the catalytic Gln69 of Ran (Bos et al., 2007; Seewald et al., 2002). Similarly, GAP$^{IP4BP}$ has been proposed to promote Rap GTP hydrolysis by repositioning a noncanonical catalytic glutamine residue, Gln63, located two positions C terminal to the position corresponding to Ras Gln61 (Sot et al., 2010). In the case of Rheb, we propose that Rheb-TSC2GAP interaction stabilizes Asp65 closer to the γ-phosphate to catalyze GTP hydrolysis in synergy with the Asn thumb (Asn1643) provided by TSC2GAP. The delineation of the precise details of TSC2-mediated catalysis will require a more detailed structural analysis of the Rheb:TSC2GAP complex that is hindered by the transient nature of their interaction observed by us and others (Marshall et al., 2009; Scrima et al., 2008), preventing us from distinguishing impaired binding from impaired catalysis.

The Tyr35-mediated autoinhibition of Rheb's GTPase reaction is necessary to maintain the appropriate level of activation of this small GTPase, and thus mTORC1 signaling, in response to growth factors. When growth factors are available, TSC2GAP activity becomes limiting, and Tyr35 inhibits GTP hydrolysis,

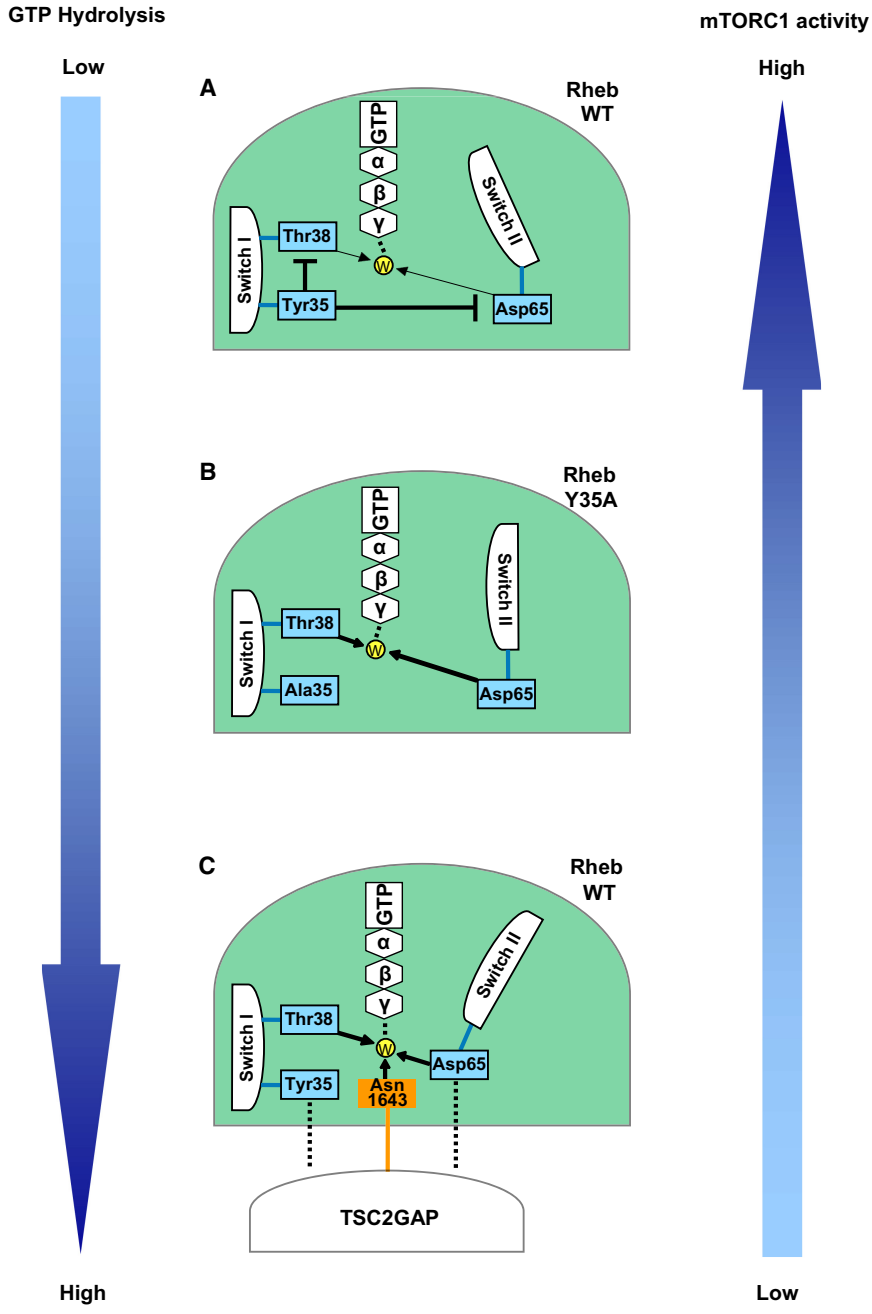


**Figure 6. Schematic Model of Intrinsic and TSC2GAP-Stimulated GTP Hydrolysis by Rheb**

(A) In WT Rheb, Tyr35 displaces the hydrolytic water away from the backbone carbonyl of Thr38, reducing the polarization and reactivity of this water molecule. Furthermore, Tyr35 reduces the electrostatic contribution of Asp65 to the GTP hydrolysis reaction by displacing this residue away from the nucleotide and the catalytic water.

(B) Mutation of Tyr35 allows Asp65 and Thr38 to assemble a more efficient catalytic site.

(C) Interaction of the GAP domain of TSC2 with Rheb may reduce the inhibitory effects of Tyr35, allowing Asp65 to promote catalysis in synergy with the Asn thumb (Asn1643) provided in *trans* by TSC2GAP.

See also Figure S6.

resulting in mTORC1 upregulation. In the absence of stimulation, Rheb Tyr35 is required for productive TSC2GAP-mediated acceleration of GTP hydrolysis to shut down mTORC1 signaling. Indeed, overexpression of Rheb Y35A substantially uncouples mTOR signaling from growth factors. In cells overexpressing WT Rheb, mTOR signaling was strongly responsive to the availability of serum and insulin, whereas this response was significantly dampened in cells overexpressing the Y35A mutant.

To our knowledge, this is the first example of a distinct mechanism of intrinsic nucleotide hydrolysis within the Ras subfamily, which may be relevant to some other Ras superfamily GTPases, particularly those that lack the canonical catalytic Gln in switch II (e.g., Rap GTPases). This study provides a view into an unusual mechanism of GTP hydrolysis by Rheb and an intriguing autoinhibitory interaction that blocks this GTPase reaction.

## EXPERIMENTAL PROCEDURES

### Protein Preparation

*Mus musculus* Rheb (residues 1–169) WT and mutants and TSC2 GAP domain (residues 1,525–1,742) were prepared according to previous protocols (Mazhab-Jafari et al., 2010). In brief the proteins were expressed in *Escherichia coli* (BL21) using pGEX2T vector, grown in minimal media supplemented with either $^{14}NH_4Cl$ or $^{15}NH_4Cl$ at 15°C with 0.25 mM IPTG. Mutagenesis was performed with the QuikChange Site-Directed Mutagenesis Kit. Small GTPase proteins expressed in *E. coli* copurified mainly as complexes with GDP nucleotide. Rheb and TSC2 proteins were initially purified using glutathione Sepharose, cleaved from the GST tag by thrombin, and further purified via Superdex 75 size exclusion chromatography. Human H-Ras (residues 1–171) and murine RhoA (residues 1–181) were expressed using pET15b and pET28, respectively, and purified by Ni-NTA followed by Superdex 75 after removal of the His tag with thrombin.

### Crystallization and Data Collection

Crystals of Rheb (residues 1–169) Y35A mutant were grown at room temperature with seeding using the hanging drop vapor diffusion method. The protein solution contained 20 mM Tris hydrochloride (Tris-HCl) (pH 8.0), 100 mM NaCl, 5 mM $MgCl_2$, and 0.02% $NaN_3$ w/v. The protein was concentrated to 870 μM, and GMPPNP was added to a final concentration of 3.8 mM. The solution was allowed to sit at room temperature for 4 hr for nucleotide exchange and then placed at 4°C overnight. Crystallization experiments were set at room temperature by mixing equal volumes of the protein solution with the well solution (100 mM Tris-HCl [pH 8.5], 200 mM sodium acetate trihydrate, and 30% w/v Polyethylene Glycol 4000). Seed crystals (grown at 4°C from a 360 μM protein

solution containing 1.56 mM GMPPNP and a well solution of 100 mM Tris-HCl [pH 8.5], 200 mM sodium acetate trihydrate, and 30% w/v Polyethylene Glycol 4000) were added in serial dilution to hanging drops to promote crystal growth. Resulting crystals were soaked in a cryoprotective solution containing 25% PEG 400 and flash frozen in liquid nitrogen. The diffraction data were collected using an R-Axis IV++, Rigaku RUH3R rotating anode generator equipped with Osmic optics and an X-stream cryosystem for data collection at a temperature of 100 K with a wavelength of 1.54 Å and processed using HKL2000 (Otwinowski and Minor, 1997).

### Structure Determination and Refinement

The phase problem was solved by molecular replacement method using the structure of WT Rheb (PDB 1XTR) as a search model. Successive rounds of refinements and manual model building were performed to construct the final model. PHENIX was used for both phase determination and structure refinement (Adams et al., 2010), whereas manual model building was performed in Coot (Emsley and Cowtan, 2004). During the course of refinement, density for the nucleotides could be clearly seen in difference electron density maps, which allowed us to manually position GMPPNP bound to one Rheb molecule and GDP bound to the other Rheb molecule in the asymmetric unit. The refinement statistic can be found in Table 1.

### NMR-Based GTPase Assays

Rheb WT and mutants were loaded with GTP or mantGTP by incubation with a 10- to 20-fold molar excess of nucleotide in the presence of 10 mM EDTA. Full nucleotide loading was confirmed by collecting a sensitivity-enhanced $^{1}H$-$^{15}N$ HSQC spectrum, and the mixture was then passed through a desalting column (PD MidiTrap G-25; GE Healthcare) equilibrated with NMR buffer (20 mM sodium phosphate [pH 7.0], 100 mM NaCl, 5 mM $MgCl_2$, 1mM DTT, and 5% $D_2O$), to produce a 1:1 complex of GTPase and the nucleotide for the kinetic measurements. Nucleotide loading of Ras was achieved by the same method; however, in the case of RhoA, 0.5 M urea was included to facilitate the EDTA-mediated nucleotide exchange and was removed by the desalting column (Mazhab-Jafari et al., 2010).

NMR experiments were run on a Bruker AVANCE II 800 MHz spectrometer equipped with a 5 mm TCI CryoProbe or a 600 MHz spectrometer equipped with TCI 1.7 mm MicroCryoProbe. Sensitivity-enhanced $^{1}H$-$^{15}N$ HSQCs with four scans (10 min) were run in succession for monitoring the GTP hydrolysis reactions at a temperature of 20°C using GTPase concentrations of 0.1–0.3 mM. The spectra were then processed with NMRPipe (Delaglio et al., 1995), and GDP- and GTP-specific peak heights were analyzed via Gaussian line fitting using SPARKY (Goddard and Kneller). Residues from switch I and II, P loop, β3 and β4, and the α3 helix that exhibit distinct well-resolved resonances in each nucleotide-bound form were used as reporters of the reaction rates, as described previously (Marshall et al., 2009; Mazhab-Jafari et al., 2010). The fraction of GTPase protein in the GDP-bound state was calculated for each reporter residue using the following equation: $I_{GDP}/(I_{GDP}+I_{GTP})$, where I represents intensity, and plotted against time. In the case of RhoA, the decay of $I_{GDP}$ peaks was used in the rate calculation, as described previously (Gasmi-Seabrook et al., 2010; Mazhab-Jafari et al., 2010). Data fitting was done using PRISM (GraphPad software). To assay GAP-mediated nucleotide hydrolysis, TSC2GAP was added to GTP-loaded Rheb at a GAP to GTPase molar ratio of 1:2.

### Thermodynamic Measurements

All assays for thermodynamic measurements of WT, Y35A, Y35F, Y35A-D65A, and D65A Rheb were run on 600 MHz spectrometer at a protein concentration of 0.5 mM in 20 mM HEPES (pH 8.0), 100 mM NaCl, 5 mM $MgCl_2$, 2 mM DTT, and 10% $D_2O$ with four scans. The GTPase assays were run at four temperatures (287, 292, 296, and 301.5 K), and Arrhenius plots were constructed by plotting ln(k) as a function of 1/T (K), where k is the rate of GTP hydrolysis in $s^{-1}$. Activation energy (Ea) and activation entropy ($\Delta S^{\ddagger}$) values were calculated from the slope and y-intercept, respectively, as described previously. The activation enthalpy ($\Delta H^{\ddagger} = Ea - RT$) and the free energy of activation ($\Delta G^{\ddagger} = \Delta H^{\ddagger} - T\,\Delta S^{\ddagger}$) were then calculated with T set to 298 K. The $\Delta G^{\ddagger}$ values are reported in kJ/mol.

### Cell-Based Phosphorylation Assay

All chemicals were purchased from Sigma-Aldrich unless stated otherwise. Antibodies against p70 S6 Kinase and p70 S6 Kinase phosphorylated at Thr389 were from Cell Signaling Technology, and Anti-Myc 9E10 is described previously by Buerger et al. (2006). Murine Rheb cDNA was obtained from Open Biosystems and subcloned into pcDNA3.1 myc-His. The Rheb mutations were generated by site-directed mutagenesis (Agilent).

HeLaBT cells were cultured in Dulbecco's modified Eagle's medium containing 10% fetal calf serum (DMEM/10% FCS) and transfected using the calcium phosphate precipitation method. Twenty-four hours after transfection, the media were replaced with serum-free DMEM. Forty-eight hours after transfection, cells were either further starved, or stimulated for 15 min or 6 hr with DMEM/10% FCS and 10 μg/ml insulin. Cells were then lysed in CHAPS lysis buffer (40 mM HEPES [pH 7.5], 0.3% CHAPS, 120 mM NaCl, 1 mM EDTA, 10 mM pyrophosphate, 50 mM NaF, 1 mM $Na_2VO_3$, 20 mM β-glycerophosphate, and protease inhibitors). Total protein in lysates was quantified using Bradford reagent (Bio-Rad), and equalized. Samples were then boiled in SDS-PAGE sample buffer, separated by SDS-PAGE, and transferred to PVDF membranes. After blocking in 5% BSA in TBS-T (50 mM Tris-HCl [pH 7.5], 150 mM NaCl, and 0.1% Tween 20), membranes were probed with the indicated antibodies and visualized with HRP-conjugated secondary antibodies using the ECL system (Amersham).

The band intensities of p70 S6K P-Thr389, total S6K, and Myc-Rheb for each lysate were measured using ImageJ software (NIH). Normalized p70 S6K P-Thr389 values were determined using the formula ((p70 S6K P-Thr389)/(total S6K))/(Myc-Rheb), and the value for Rheb WT under growth factor-stimulated condition was set to 100 for each time point after starvation/stimulation.

### Nucleotide Binding In Vivo

Labeling was done according to previous protocols by Wolthuis et al. (1997) with the following modification. HEK293 cells were seeded in a 6-well plate and transfected with 2.5 μg of DNA using the calcium-phosphate method. The following morning, cells were washed and maintained in DMEM containing 10% FBS, and 6 hr later, their media were replaced with phosphate- and serum-free DMEM and the cells incubated for 1 hr. Cells were labeled with 250 μCi/ml of [$^{32}$P]orthophosphoric acid (PerkinElmer) overnight. Cells were washed with cold PBS and lysed in 750 μl of 50 mM Tris (pH 7.4), 140 mM NaCl, 1 mM KCl, 2 mM $MgCl_2$, 1% Triton X-100, protease inhibitor cocktail. Lysates were precleared with 20 μl of protein A Sepharose for 20 min. Myc-Rheb was immunoprecipitated with 1 μg of anti-myc antibody (Cell Signaling) for 2 hr and 20 μl of protein A Sepharose for 30 min. Immunoprecipitates were washed four times in lysis buffer containing 500 mM NaCl and twice in lysis buffer with 0.1% Triton X-100. Nucleotides were eluted in 20 μl of 2 mM EDTA, 2 mM DTT, 0.2% SDS, 1 mM GDP, 1 mM GTP at 68°C for 15 min. Eluted nucleotides were separated by spotting 10 μl on PEI cellulose TLC plates and resolved in 0.75 M $KH_2PO_4$ (pH 3.4). Air-dried TLC plates were exposed using a phosphorimager and GTP/GDP ratios calculated using ImageQuant 5.2 software.

## ACCESSION NUMBERS

The PDB accession number for the Rheb Y35A structures reported in this paper is 3SEA.

## SUPPLEMENTAL INFORMATION

Supplemental Information includes seven figures, one table, and Supplemental Experimental Procedures and can be found with this article online at http://dx.doi.org/10.1016/j.str.2012.06.013.

## ACKNOWLEDGMENTS

This work was supported by the Cancer Research Society (Canada), Canadian Cancer Society Research Institute Grant #2010-700494, and a U.S. Department of Defense Tuberous Sclerosis Complex Research Program Award to V.S. The 800 and 600 MHz NMR spectrometers were funded by the Canada Foundation for Innovation. We thank L. Howell (HSC Toronto) for the use of the X-ray facility. M.T.M.J. was supported by NSERC. M.I. holds Canada

Research Chair, and V.S. holds an Early Researcher Award from the Government of Ontario.

Received: October 25, 2011
Revised: June 18, 2012
Accepted: June 20, 2012
Published online: July 19, 2012

## REFERENCES

Adams, P.D., Afonine, P.V., Bunkóczi, G., Chen, V.B., Davis, I.W., Echols, N., Headd, J.J., Hung, L.W., Kapral, G.J., Grosse-Kunstleve, R.W., et al. (2010). PHENIX: a comprehensive Python-based system for macromolecular structure solution. Acta Crystallogr. D Biol. Crystallogr. *66*, 213–221.

Allin, C., Ahmadian, M.R., Wittinghofer, A., and Gerwert, K. (2001). Monitoring the GAP catalyzed H-Ras GTPase reaction at atomic resolution in real time. Proc. Natl. Acad. Sci. USA *98*, 7754–7759.

Benvenuto, G., Li, S., Brown, S.J., Braverman, R., Vass, W.C., Cheadle, J.P., Halley, D.J., Sampson, J.R., Wienecke, R., and DeClue, J.E. (2000). The tuberous sclerosis-1 (TSC1) gene product hamartin suppresses cell growth and augments the expression of the TSC2 product tuberin by inhibiting its ubiquitination. Oncogene *19*, 6306–6316.

Bos, J.L., Rehmann, H., and Wittinghofer, A. (2007). GEFs and GAPs: critical elements in the control of small G proteins. Cell *129*, 865–877.

Brinkmann, T., Daumke, O., Herbrand, U., Kühlmann, D., Stege, P., Ahmadian, M.R., and Wittinghofer, A. (2002). Rap-specific GTPase activating protein follows an alternative mechanism. J. Biol. Chem. *277*, 12525–12531.

Brucker, S., Gerwert, K., and Kötting, C. (2010). Tyr39 of ran preserves the Ran.GTP gradient by inhibiting GTP hydrolysis. J. Mol. Biol. *401*, 1–6.

Buerger, C., DeVries, B., and Stambolic, V. (2006). Localization of Rheb to the endomembrane is critical for its signaling function. Biochem. Biophys. Res. Commun. *344*, 869–880.

Buhrman, G., Holzapfel, G., Fetics, S., and Mattos, C. (2010). Allosteric modulation of Ras positions Q61 for a direct role in catalysis. Proc. Natl. Acad. Sci. USA *107*, 4931–4936.

Cepus, V., Scheidig, A.J., Goody, R.S., and Gerwert, K. (1998). Time-resolved FTIR studies of the GTPase reaction of H-ras p21 reveal a key role for the beta-phosphate. Biochemistry *37*, 10263–10271.

Cherfils, J., Ménétrey, J., Le Bras, G., Janoueix-Lerosey, I., de Gunzburg, J., Garel, J.R., and Auzat, I. (1997). Crystal structures of the small G protein Rap2A in complex with its substrate GTP, with GDP and with GTPgammaS. EMBO J. *16*, 5582–5591.

Chong-Kopera, H., Inoki, K., Li, Y., Zhu, T., Garcia-Gonzalo, F.R., Rosa, J.L., and Guan, K.L. (2006). TSC1 stabilizes TSC2 by inhibiting the interaction between TSC2 and the HERC1 ubiquitin ligase. J. Biol. Chem. *281*, 8313–8316.

Delaglio, F., Grzesiek, S., Vuister, G.W., Zhu, G., Pfeifer, J., and Bax, A. (1995). NMRPipe: a multidimensional spectral processing system based on UNIX pipes. J. Biomol. NMR *6*, 277–293.

Du, X., Frei, H., and Kim, S.H. (2000). The mechanism of GTP hydrolysis by Ras probed by Fourier transform infrared spectroscopy. J. Biol. Chem. *275*, 8492–8500.

Dunlop, E.A., Dodd, K.M., Seymour, L.A., and Tee, A.R. (2009). Mammalian target of rapamycin complex 1-mediated phosphorylation of eukaryotic initiation factor 4E-binding protein 1 requires multiple protein-protein interactions for substrate recognition. Cell. Signal. *21*, 1073–1084.

Emsley, P., and Cowtan, K. (2004). Coot: model-building tools for molecular graphics. Acta Crystallogr. D Biol. Crystallogr. *60*, 2126–2132.

Eom, M., Han, A., Yi, S.Y., Shin, J.J., Cui, Y., and Park, K.H. (2008). RHEB expression in fibroadenomas of the breast. Pathol. Int. *58*, 226–232.

Focia, P.J., Shepotinovskaya, I.V., Seidler, J.A., and Freymann, D.M. (2004). Heterodimeric GTPase core of the SRP targeting complex. Science *303*, 373–377.

Fraser, J.S., van den Bedem, H., Samelson, A.J., Lang, P.T., Holton, J.M., Echols, N., and Alber, T. (2011). Accessing protein conformational ensembles using room-temperature X-ray crystallography. Proc. Natl. Acad. Sci. USA *108*, 16247–16252.

Frech, M., Darden, T.A., Pedersen, L.G., Foley, C.K., Charifson, P.S., Anderson, M.W., and Wittinghofer, A. (1994). Role of glutamine-61 in the hydrolysis of GTP by p21H-ras: an experimental and theoretical study. Biochemistry *33*, 3237–3244.

Garami, A., Zwartkruis, F.J., Nobukuni, T., Joaquin, M., Roccio, M., Stocker, H., Kozma, S.C., Hafen, E., Bos, J.L., and Thomas, G. (2003). Insulin activation of Rheb, a mediator of mTOR/S6K/4E-BP signaling, is inhibited by TSC1 and 2. Mol. Cell *11*, 1457–1466.

Gasmi-Seabrook, G.M., Marshall, C.B., Cheung, M., Kim, B., Wang, F., Jang, Y.J., Mak, T.W., Stambolic, V., and Ikura, M. (2010). Real-time NMR study of guanine nucleotide exchange and activation of RhoA by PDZ-RhoGEF. J. Biol. Chem. *285*, 5137–5145.

Goddard, T.D., and Kneller, D. SPARKY 3 (San Francisco: University of California).

Grant, B.J., Gorfe, A.A., and McCammon, J.A. (2009). Ras conformational switching: simulating nucleotide-dependent conformational transitions with accelerated molecular dynamics. PLoS Comput. Biol. *5*, e1000325.

Im, E., von Lintig, F.C., Chen, J., Zhuang, S., Qui, W., Chowdhury, S., Worley, P.F., Boss, G.R., and Pilz, R.B. (2002). Rheb is in a high activation state and inhibits B-Raf kinase in mammalian cells. Oncogene *21*, 6356–6365.

Inoki, K., Li, Y., Xu, T., and Guan, K.L. (2003). Rheb GTPase is a direct target of TSC2 GAP activity and regulates mTOR signaling. Genes Dev. *17*, 1829–1834.

Ito, Y., Yamasaki, K., Iwahara, J., Terada, T., Kamiya, A., Shirouzu, M., Muto, Y., Kawai, G., Yokoyama, S., Laue, E.D., et al. (1997). Regional polysterism in the GTP-bound form of the human c-Ha-Ras protein. Biochemistry *36*, 9109–9119.

Jiang, H., and Vogt, P.K. (2008). Constitutively active Rheb induces oncogenic transformation. Oncogene *27*, 5729–5740.

Kötting, C., and Gerwert, K. (2004). Time-resolved FTIR studies provide activation free energy, activation enthalpy and activation entropy for GTPase reactions. Chem. Phys. *307*, 227–232.

Krengel, U., Schlichting, I., Scherer, A., Schumann, R., Frech, M., John, J., Kabsch, W., Pai, E.F., and Wittinghofer, A. (1990). Three-dimensional structures of H-ras p21 mutants: molecular basis for their inability to function as signal switch molecules. Cell *62*, 539–548.

Li, G., and Zhang, X.C. (2004). GTP hydrolysis mechanism of Ras-like GTPases. J. Mol. Biol. *340*, 921–932.

Li, Y., Inoki, K., and Guan, K.L. (2004). Biochemical and functional characterizations of small GTPase Rheb and TSC2 GAP activity. Mol. Cell. Biol. *24*, 7965–7975.

Long, X., Lin, Y., Ortiz-Vega, S., Busch, S., and Avruch, J. (2007). The Rheb switch 2 segment is critical for signaling to target of rapamycin complex 1. J. Biol. Chem. *282*, 18542–18551.

Maegley, K.A., Admiraal, S.J., and Herschlag, D. (1996). Ras-catalyzed hydrolysis of GTP: a new perspective from model studies. Proc. Natl. Acad. Sci. USA *93*, 8160–8166.

Marshall, C.B., Ho, J., Buerger, C., Plevin, M.J., Li, G.Y., Li, Z., Ikura, M., and Stambolic, V. (2009). Characterization of the intrinsic and TSC2-GAP-regulated GTPase activity of Rheb by real-time NMR. Sci. Signal. *2*, ra3.

Mazhab-Jafari, M.T., Marshall, C.B., Smith, M., Gasmi-Seabrook, G.M., Stambolic, V., Rottapel, R., Neel, B.G., and Ikura, M. (2010). Real-time NMR study of three small GTPases reveals that fluorescent 2′(3′)-O-(N-methylanthraniloyl)-tagged nucleotides alter hydrolysis and exchange kinetics. J. Biol. Chem. *285*, 5132–5136.

Nardella, C., Chen, Z., Salmena, L., Carracedo, A., Alimonti, A., Egia, A., Carver, B., Gerald, W., Cordon-Cardo, C., and Pandolfi, P.P. (2008). Aberrant Rheb-mediated mTORC1 activation and Pten haploinsufficiency are cooperative oncogenic events. Genes Dev. *22*, 2172–2177.

Otwinowski, Z., and Minor, W. (1997). Processing of X-ray diffraction data collected in oscillation mode. Methods Enzymol. *276*, 307–326.

 

Scheffzek, K., Ahmadian, M.R., Kabsch, W., Wiesmüller, L., Lautwein, A., Schmitz, F., and Wittinghofer, A. (1997). The Ras-RasGAP complex: structural basis for GTPase activation and its loss in oncogenic Ras mutants. Science *277*, 333–338.

Scheidig, A.J., Franken, S.M., Corrie, J.E., Reid, G.P., Wittinghofer, A., Pai, E.F., and Goody, R.S. (1995). X-ray crystal structure analysis of the catalytic domain of the oncogene product p21H-ras complexed with caged GTP and mant dGppNHp. J. Mol. Biol. *253*, 132–150.

Scrima, A., Thomas, C., Deaconescu, D., and Wittinghofer, A. (2008). The Rap-RapGAP complex: GTP hydrolysis without catalytic glutamine and arginine residues. EMBO J. *27*, 1145–1153.

Seewald, M.J., Körner, C., Wittinghofer, A., and Vetter, I.R. (2002). RanGAP mediates GTP hydrolysis without an arginine finger. Nature *415*, 662–666.

Sot, B., Kötting, C., Deaconescu, D., Suveyzdis, Y., Gerwert, K., and Wittinghofer, A. (2010). Unravelling the mechanism of dual-specificity GAPs. EMBO J. *29*, 1205–1214.

Tee, A.R., Manning, B.D., Roux, P.P., Cantley, L.C., and Blenis, J. (2003). Tuberous sclerosis complex gene products, Tuberin and Hamartin, control mTOR signaling by acting as a GTPase-activating protein complex toward Rheb. Curr. Biol. *13*, 1259–1268.

Wennerberg, K., Rossman, K.L., and Der, C.J. (2005). The Ras superfamily at a glance. J. Cell Sci. *118*, 843–846.

Wolthuis, R.M., de Ruiter, N.D., Cool, R.H., and Bos, J.L. (1997). Stimulation of gene induction and cell growth by the Ras effector Rlf. EMBO J. *16*, 6748–6761.

Yamagata, K., Sanders, L.K., Kaufmann, W.E., Yee, W., Barnes, C.A., Nathans, D., and Worley, P.F. (1994). rheb, a growth factor- and synaptic activity-regulated gene, encodes a novel Ras-related protein. J. Biol. Chem. *269*, 16333–16339.

Yu, Y., Li, S., Xu, X., Li, Y., Guan, K., Arnold, E., and Ding, J. (2005). Structural basis for the unique biological function of small GTPase RHEB. J. Biol. Chem. *280*, 17093–17100.